

# Two-dimensional and Three-dimensional Resistivity Imaging in Archaeological Site Investigation

N. G. PAPADOPOULOS,<sup>1,2\*</sup> P. TSOURLOS,<sup>1</sup> G. N. TSOKAS<sup>1</sup> AND A. SARRIS<sup>2</sup>

<sup>1</sup> Department of Geophysics, School of Geology, Aristotle University of Thessaloniki, 54124, Thessaloniki, Greece

<sup>2</sup> Laboratory of Geophysical-Satellite Remote Sensing and Archaeo-environment, Institute for Mediterranean Studies, Foundation of Research and Technology-Hellas, P.O. Box 119, Rethymnon, 74100, Crete, Greece

**ABSTRACT** In this work, the application and the effectiveness of two- and three-dimensional non-linear inversion algorithms in processing and interpretation of electrical resistivity tomography (ERT) data collected from archaeological areas are investigated in the framework of a new field technique for gathering three-dimensional pole–pole tomographic data in a relatively small amount of time using standard archaeological prospection equipment. The inversion routine, for both the two-dimensional and the three-dimensional case, is based on a smoothness constrained algorithm and the forward modelling calculations are carried out using two-dimensional and three-dimensional finite element solvers respectively. Results of combined two-dimensional inversions (quasi-three-dimensional) are compared with the full three-dimensional inversions. Comparisons are carried out in relation to the optimum survey direction of gathering the tomographic data using the pole–pole array for synthetic data arising from three-dimensional structures commonly encountered in archaeological sites. The response of the algorithms in the presence of noisy data was also tested. The algorithms were also used in the processing of real data collected from the archaeological sites of Sikyon and Europos in Greece. The results from the synthetic and the real data indicate the superiority of the three-dimensional inversion algorithms in processing tomographic data. The reconstructed three-dimensional images do not suffer from the artefacts encountered in the quasi-three-dimensional approach, owing to the three-dimensional nature of the archaeological features. Most importantly, both synthetic and real data results indicate that a single survey direction is adequate to produce a valid three-dimensional subsurface image when full three-dimensional inversion is used in contrast to the quasi-three-dimensional approach, which would require that two survey directions be used to obtain satisfactory results. Copyright © 2006 John Wiley & Sons, Ltd.

*Key words:* two-dimensional ERT inversion; three-dimensional ERT inversion; Quasi-three-dimensional ERT inversion; resistivity survey technique

## Introduction

The electrical resistivity tomography (ERT) technique is considered a relatively new geophysical

method, which has evolved rapidly over the past 10 yr. The electrical resistivity method is widely used in the investigation and detection of shallow-depth targets. The method aims to determine the variation of the subsurface resistivity by conducting measurements at the ground surface or inside shallow boreholes. The electrical method has been applied with great success in solving hydrogeological (Flathe, 1955; Dahlin

\*Correspondence to: N. G. Papadopoulos, Department of Geophysics, School of Geology, Aristotle University of Thessaloniki, 54124, Thessaloniki, Greece.  
E-mail: nikos@ims.forth.gr

and Owen, 1998), geological (Caglar and Duvarci, 2001; Atzemoglou *et al.*, 2003), engineering (Dahlin *et al.*, 1994) and environmental problems (Rogers and Kean, 1980; Van *et al.*, 1991; Ramirez *et al.*, 1996).

The development of the technology associated with automatically multiplexed electrode arrangements and automatic measuring systems facilitate the acquisition of a large number of measurements in a limited time. Further, the advent of fast computers allowed the development of automated resistivity inversion schemes, which aim to construct an estimate of a subsurface resistivity distribution that is consistent with the experimental data. Among others, the smoothness constraint inversion (Constable *et al.*, 1987) has become a popular technique for interpreting ERT data because it produces a simplified subsurface resistivity model that is a reasonable representation of the subsurface and at the same time guarantees inversion stability. Several two-dimensional smoothness constrained inversion algorithms for ERT data have been presented in the literature (Sasaki, 1992; Xu and Noel, 1993; Ellis and Oldenburg, 1994; Loke and Barker, 1995; Tsourlos, 1995). Further, as many of the problems associated with geophysical exploration are of a three-dimensional nature several algorithms for treating the ERT problem in three-dimensions have been presented (e.g. Park and Van, 1991; Loke and Barker, 1996; Tsourlos and Ogilvy, 1999).

Despite the development of advanced instrumentation and three-dimensional interpretation techniques, common geophysical practice still relies mainly on two-dimensional approaches, both in view of measurements and interpretations (Chambers, 2001). Dense two-dimensional measurements are routinely being interpreted with two-dimensional algorithms and the results are combined a-posteriori to generate quasi-three-dimensional ( $x,y,z$ ) images. This type of result often suffers from artefacts, either due to the fact that three-dimensional responses are attributed to two-dimensional structures or due to the varying level of misfit that individual two-dimensional inversions may reach (Dahlin and Loke, 1997).

The resistivity technique is very popular in the investigation of archaeological sites for mapping buried antiquities. The success of the method

depends on the different resistivity properties between the potential archaeological targets (walls, roads, buildings, ditches) and the surrounding environment.

A number of electrode arrays, such as Wenner and Schlumberger configurations, are used in the resistivity investigation of archaeological sites. Aspinall and Gaffney (2001) discussed the potential and pitfalls of the Schlumberger array in archaeological prospection. The results confirmed the high selectivity of the array response to the orientation of the feature, as structures parallel to the array orientation were poorly recognized. Additionally the vertical geoelectrical sounding technique was proved to be very promising for the exploration of buried archaeological targets (Gaber *et al.*, 1999; Chouker, 2001).

Nowadays the twin-probe array is the most popular and is used routinely in the geophysical mapping of archaeological sites (Clark, 1990). The implementation of the specific configuration is very easy as only two electrodes (one current and one potential electrode) have to be moved at each station, while two other (one current and one potential) probes stay fixed and close to each other, at a great distance from the survey area. Additionally it gives a strong and clear response over archaeological features, that is easy to interpret. The resistivity mapping of specific areas with this particular array has been used with great success to delineate the plan view of buried archaeological structures in various cases (Sarris, 1992; Tsokas *et al.*, 1994; Sarris *et al.*, 2002).

The development of mobile arrays has increased the area coverage, reducing dramatically the time taken to conduct the survey (Panissod *et al.*, 1998; Dabas *et al.*, 2000). Furthermore the use of multiplexing systems has aided the determination of the apparent resistivity distribution in three-dimensions (Walker, 2000).

Electrical resistivity tomography was first used for imaging archaeological structures in a trial survey at Verulamium, St Albans (Noel, 1991). In archaeological prospection, electrical tomography is used mainly as a complementary tool to enhance the information context gained from other geophysical methods. A number of

case studies of the method have been reported in the literature (Neighbour *et al.*, 2001; Dogan and Papamarinopoulos, 2003; Rizzo *et al.*, 2005). Furthermore, full three-dimensional electrical resistivity measurements have also been applied experimentally in the investigation of an archaeological site in Lasithi, Greece (Vafidis *et al.*, 1999).

## Two- and three-dimensional measuring modes

The two-dimensional electrical resistivity tomography can be defined as the collection of a number of profiles in an area, with continuously increasing inner-electrode spacing or as a series of successive electrical soundings along a line. Practically, a number of equally spaced electrodes are inserted into the ground along a profile and various measurements are obtained for varying electrode spacing so as to record the horizontal and vertical variation of the subsurface resistivity.

Nowadays two-dimensional resistivity measurements are quite easy, low in cost and fast to implement, as new, advanced and fully automated resistivity instruments have been developed. Furthermore the development of two-dimensional inversion resistivity algorithms has aided to the processing and interpretation of such complicated data. The two-dimensional measuring mode gives satisfactory and trustworthy results in cases where the strike of subsurface concealed bodies extend to a practically infinite distance, vertical to the electrical tomography direction. In cases of complex geology, artefacts may be generated in the two-dimensional sections owing to the three-dimensional nature of the underground structures.

In order to overcome the above-mentioned problem, full three-dimensional measurements of the resistivity must be considered. The electrodes are normally arranged in a rectangular grid with the same unit electrode spacing in the  $X$  and  $Y$  direction (Loke and Barker, 1996). In this case each electrode is used as a current electrode and the potentials are measured at all the other

electrodes. Due to the reciprocity, it is only necessary to measure the potential at the electrodes with higher index number than the current electrode (Fig. 1A).

In the three-dimensional surveys the pole–pole configuration is commonly used. The maximum number of independent measurements that can be made with  $P$  electrodes is  $n_{\max} = P(P - 1)/2$  (Xu and Noel, 1993). For example, if the rectangular grid of Figure 1A is considered, where 24 electrodes are used, then with the pole–pole configuration a complete data set will have 276 datum points. It is obvious that it will be very time consuming to gather such complete sets of three-dimensional measurements using typical single-channel resistivity meters.

Nowadays multichannel automated resistivity meters have been developed reducing the overall time taken to collect such data. Again the time needed has not reduced to an acceptable level to be able to conduct such surveys on a routine basis. So even today the most common practice to record the three-dimensional resistivity variation of the subsurface is to gather dense, parallel two-dimensional lines with the interline spacing equal to the basic interelectrode spacing. The data can be collected parallel to the  $X$  axis ( $X$  survey), or parallel to the  $Y$  axis ( $Y$  survey) or parallel to both axes ( $XY$  survey). The three different strategy modes to collect three-dimensional data can be seen in Figure 1B. The synthetic and the real data used in this work were collected following this strategy.

Parallel two-dimensional tomographies are routinely interpreted using two-dimensional inversion algorithms and the outcome results are combined to create a quasi-three-dimensional ( $x, y, z$ ) image of the subsurface resistivity distribution. This type of result often suffers from artefacts, either due to the fact that three-dimensional responses are attributed to two-dimensional structures or due to the varying level of misfit that individual two-dimensional inversions may reach. It is therefore reasonable to assume that the quality of the quasi-three-dimensional images depends on the degree of noise of the measurements and the complicated nature of the subsurface structure. The main goal of this work, therefore, is to investigate the application and the effectiveness of full

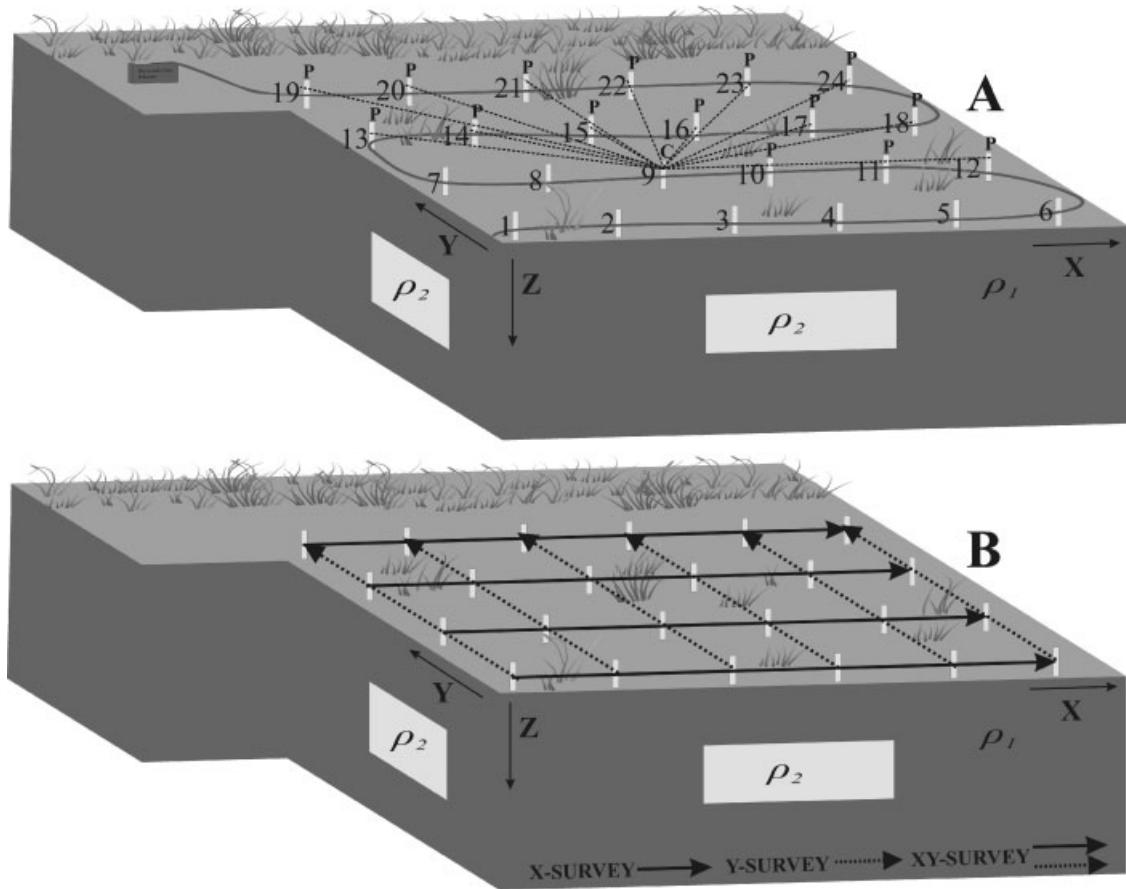


Figure 1. (A) Arrangement of 24 electrodes in a  $6 \times 4$  units rectangular grid in order to measure the three-dimensional resistivity distribution of the subsurface. P and C stand for potential and current electrode respectively. (B) The three different measuring modes followed in this work. X survey (two-dimensional measurements parallel to the X axis), Y survey (two-dimensional measurements parallel to the Y axis) and XY survey (two-dimensional measurements parallel to both axes).

three-dimensional inversion algorithms in the processing of such dense two-dimensional data and examine the differences between the quasi-three-dimensional and real-three-dimensional images.

## Modelling and inversion

The response of the three-dimensional models used in this work was calculated using the finite element method (FEM). In every inversion algorithm (either two-dimensional or three-dimensional) the routine solving the forward resistivity problem is an essential part of the processing procedure. The technique has been described extensively in many works (Coggon,

1971; Rijo, 1977, Pridmore *et al.*, 1981; Tsourlos and Ogilvy, 1999; Tsourlos *et al.*, 1999), so only a brief outline is presented here.

### 2.5-dimensional FEM modelling

In the 2.5-dimensional resistivity modelling the current flow pattern is considered to be three-dimensional whereas the change in resistivity is two-dimensional. In other words, the measured potential values correspond to a three-dimensional subsurface where the resistivity is allowed to vary in only two dimensions and remains constant in the strike direction. 2.5-dimensional modelling provides accurate results as long as the two-dimensional resistivity variation assumption is not strongly violated. In order to

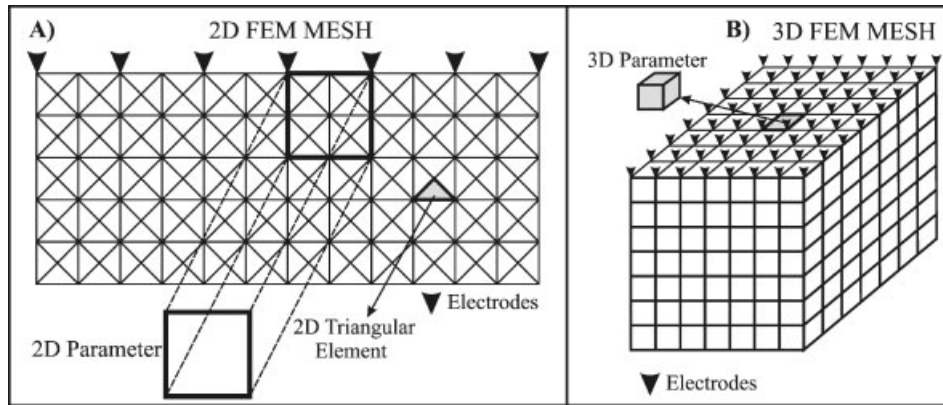


Figure 2. (A) Division of the subsurface into triangular elements for the two-dimensional forward modelling case (Tsourlos, 1995). (B) Use of three-dimensional hexahedral elements to discretize the domain for the three-dimensional case (Tsourlos and Ogilvy, 1999).

include the potential variability in the strike ( $y$ ) direction a cosine Fourier transformation is applied, by solving the problem for many different wavenumbers.

In the FEM framework the earth is divided into a finite number of homogeneous triangular (in this case) subdomains, which are called elements (Figure 2A). These elements are connected at common nodal points and approximate the shape of the region. The potential within each element is approximated by a simple interpolation function (basis function) and is calculated in specific points of the mesh known as nodes. In order to minimize the error between the approximated and the real potential, the Galerkin minimization criterion is applied (Burnett, 1988). After applying the Galerkin minimization scheme to every element, the individual element equations are converted to element matrix equations and then the matrix element equations can be assembled into one global system, which has the following form

$$\mathbf{KA} = \mathbf{F} \quad (1)$$

where  $\mathbf{K}$  is the stiffness matrix, which is related to the nodal coordinates,  $\mathbf{A}$  is the unknown transformed nodal potential vector and  $\mathbf{F}$  is the vector describing the sources. After applying the boundary conditions, the system of equation (1) is solved for several wavenumbers and the transformed nodal potential is obtained by applying the inverse Fourier transform. As the nodal

potential is known, the point to point potential differences and the apparent resistivities calculation is straightforward.

#### Three-dimensional FEM modelling

In order to solve the three-dimensional forward resistivity problem, an approach similar the 2.5-dimensional case is followed. The subsurface is now discretized into hexahedral elements (Figure 2B) and again the Galerkin minimization method is applied in order to minimize the error between the true and the approximated potential. The matrix element equations are assembled into a global system that has the same form of equation (1). Then the boundary conditions are applied and the system (equation 1) is solved once to calculate the nodal potential.

#### Inversion

Generally the application of the inversion theory in the geoelectrical investigation tries to find the optimum electric model of the ground for which its response, calculated using the forward modelling procedure, will be similar to or almost the same as the real (observed) apparent resistivity data in view of the data uncertainties. During the reconstruction procedure the subsurface is divided into smaller regions, called parameters, which are allowed to vary their resistivity independently.

As the electrical inverse problem is non-linear, the above procedure has to be iterative. Usually the inversion procedure begins with a starting model of the ground (homogeneous ground) and a resistivity correction model is found in every iteration. This correction vector is then added to the previous model. Thus, at the end of every inversion an upgraded model of the ground is received and finally the procedure will stop when the root mean square error between real and calculated apparent resistivities is practically stable.

The inversion routine of the program is the same for both the two-dimensional and three-dimensional cases. The inversion is based on a non-linear smoothness constrained algorithm (Sasaki, 1992). The resistivity estimate  $\mathbf{x}_{k+1}$  at the  $k+1$ th iteration is given by

$$\begin{aligned}\mathbf{x}_{k+1} &= \mathbf{x}_k + d\mathbf{x}_k \\ &= \mathbf{x}_k + [(\mathbf{J}_k^T \mathbf{J}_k + \lambda_k \mathbf{C}^T \mathbf{C})]^{-1} \mathbf{J}_k^T [\mathbf{y} - \mathbf{F}(\mathbf{x}_k)]\end{aligned}\quad (2)$$

where  $\mathbf{y}$  is the measured data vector,  $\mathbf{J}_k$  is the Jacobian matrix estimate of the  $\mathbf{x}_k$  resistivity distribution,  $d\mathbf{x}_k$  is the resistivity correction vector,  $\mathbf{F}(\mathbf{x}_k)$  is the forward modelling operator,  $\mathbf{C}$  is the matrix that describes the smoothness pattern of the model (de Groot-Hedlin and Constable, 1990) and  $\lambda_k$  the Lagrangian multiplier. Super-script T denotes the transpose matrix.

The smoothness-constrained inversion tries to find the simplest and smoothest resistivity model of the earth. It does not necessarily seek the 'best' solution but it is hoped that the model produced will be a reasonable representation of the earth. Namely, this type of inversion guarantees the stability of the solution.

The adjoint equation approach (McGillivray and Oldenburg, 1990) was incorporated into the FEM scheme in order to calculate the Jacobian matrix  $\mathbf{J}$  (Tsourlos, 1995; Tsourlos and Ogilvy, 1999). Depending on the dimension of the problem the Jacobian matrix is calculated either by the 2.5-dimensional or the three-dimensional forward solver. Additionally the Singular Value Decomposition (SVD) method (Press *et al.*, 1992) was used to invert the matrix during the inversion procedure in the two-dimensional case. In contrast an iterative technique Least Squares Regression (LSQR) (Paige and Saunders, 1982)

was used to solve the large sparse linear systems that result in the three-dimensional inversion procedure.

## Instrumentation

A modified data collection technique to gather tomographic resistivity data in a relatively small amount of time using the Geoscan RM15 soil resistance meter was implemented. The Geoscan RM15 soil resistance meter, the Multiplexer MPX15 and the multiprobe frame PA5 were appropriately configured and programmed to conduct the survey with the pole-pole array. Five probes were placed on the frame. One of them was always used as the current electrode A, whereas the remaining four probes (M1, M2, M3 and M4) were used to measure the potential. The distance between the pair of electrodes A-M1, A-M2, A-M3 and A-M4 was 0.5 m, 1 m, 1.5 m and 2 m respectively (Figure 3 top). Two extra 50-m cables were used to separate the remote electrodes (B, N) at a sufficient distance (almost infinite) between them, so that the distance between them was effectively infinite (Figure 3 bottom).

The tomographies parallel to the  $x$  axis were completed by moving the frame and the RM15\MPX15 system along the  $Y$  axis in a parallel mode, whereas those parallel to  $Y$  axis were conducted by moving the instrument along the  $X$  axis (Figure 3 bottom). The interline spacing was 0.5 m for both the surveys.

## Synthetic data

The synthetic data created in this study were based on the specific properties and limitations that characterized the resistance instrument used to gather the real data. Synthetic data were created assuming that 20 two-dimensional lines parallel to the  $X$  axis and 20 two-dimensional lines parallel to the  $Y$  axis were obtained with the pole-pole array. The interline and interelectrode spacing was  $a = 1$  m or  $a = 0.5$  m, depending on the model used, while the maximum number of the recorded depth layers was set equal to four ( $n_{\max} = 4a$ ).

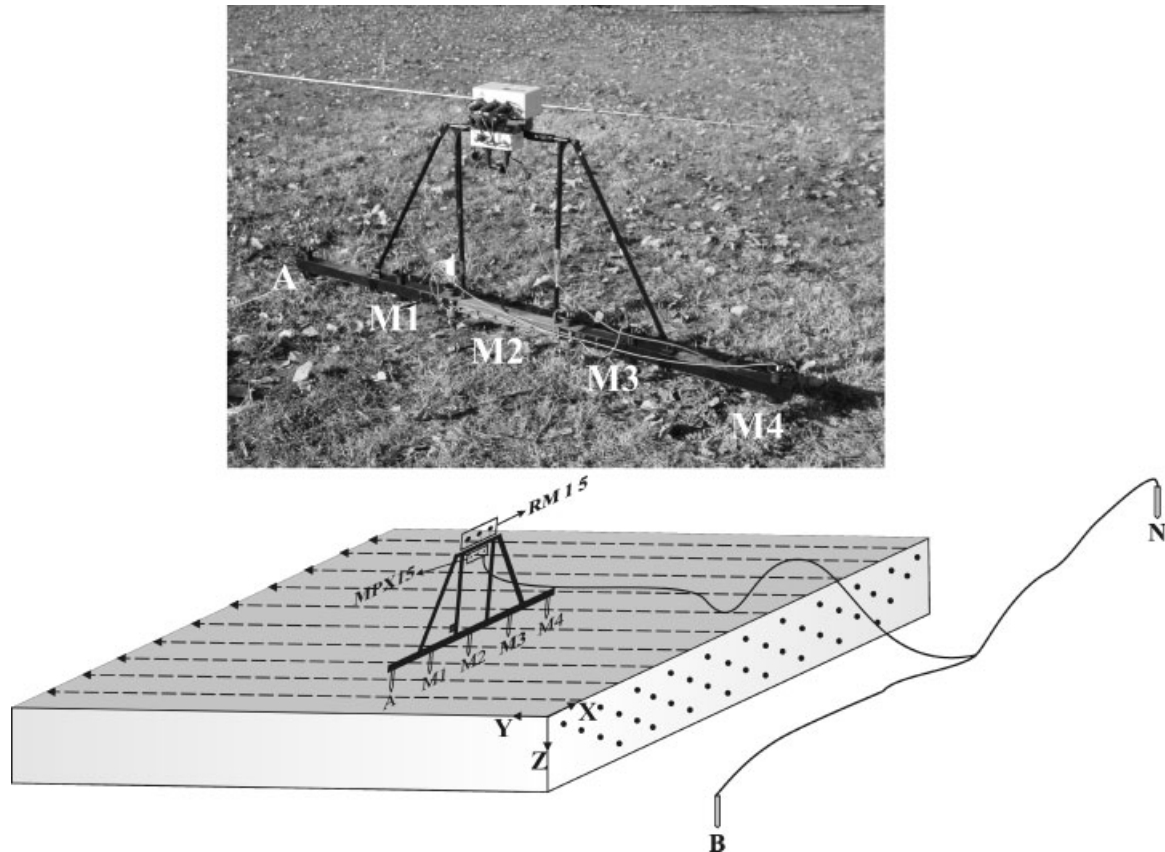


Figure 3. (top) Connection of the RM15 resistance meter with the multiplexer MPX15 and the multiprobe frame PA5, where the interelectrode distance of A–M1, A–M2, A–M3 and A–M4 is 0.5, 1, 1.5 and 2 m respectively. (bottom) The movement of the instrument to a field layout mode adequate to complete the two-dimensional lines parallel to the X axis.

A three-dimensional forward algorithm was used to calculate the synthetic apparent resistivities produced by the three-dimensional bodies (Tsourlos and Ogilvy, 1999). Three-dimensional rectangular shaped models, which mainly appear in the archaeological sites, were considered in this study. Furthermore, the synthetic data were contaminated with Gaussian noise (Press *et al.*, 1992) in order to investigate the effectiveness of the algorithms in the presence of noisy data.

The first model consists of two prismatic structures. Such three-dimensional features are the most common archaeological targets, as they may represent buried walls or building remnants. The two features were given resistivity of  $100 \Omega\text{-m}$ , where the background resistivity was

set equal to  $10 \Omega\text{-m}$  and they were considered at a depth of 0.5–1.0 m (Figure 4A).

Each resistivity tomography, along X and Y axes, was processed and inverted separately using a two-dimensional inversion algorithm. Afterwards the interpreted two-dimensional sections were combined to produce quasi-three-dimensional depth slices of the resistivity distribution for the X, Y and XY direction (Figure 4C). Additionally the three-dimensional distribution of the calculated apparent resistivities caused by the two prismatic bodies, parallel to X and parallel to XY axes, has also been plotted in Figure 4B.

It is obvious from Figure 4A and B that although the modelling bodies were placed at a depth of 0.5–1.0 m, the apparent resistivities

**MODEL 1**

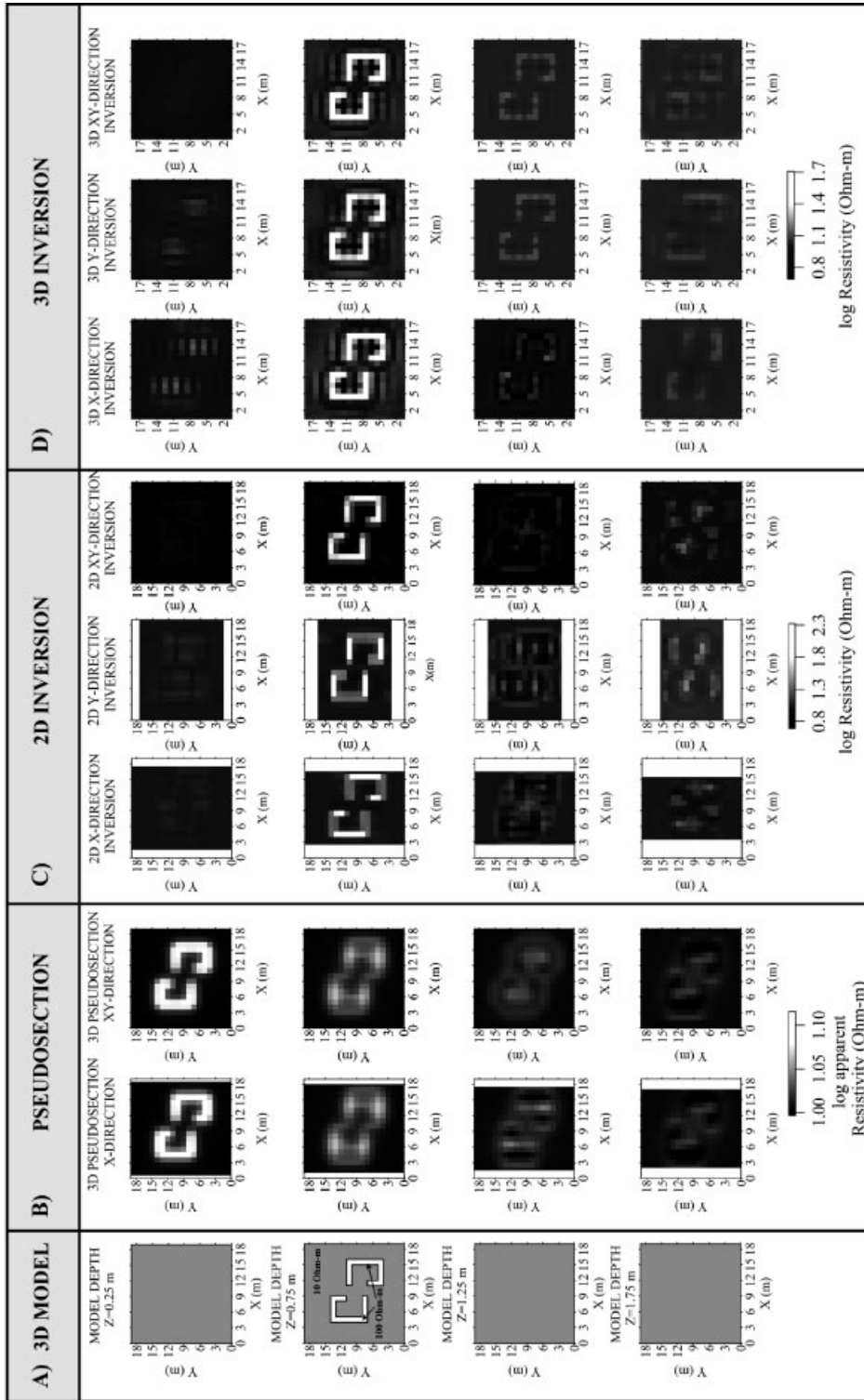


Figure 4. (A) Three-dimensional resistivity model 1. (B) Three-dimensional distribution of the calculated apparent resistivities resulted from model 1. (C) Quasi-three-dimensional resistivity model resulting from the two-dimensional inversions along the X, Y and XY axes. (D) three-dimensional resistivity model derived from the three-dimensional inversion. The logarithm of the resistivity has been plotted.

depth slices indicate that the two bodies seem to be buried at a depth from 0 to 0.5 m. So, if the interpretation was to be based on the apparent resistivity depth slices, then the outline of the structures is well delineated but the three-dimensional pseudosections provide an erroneous estimate of the true burial depth.

Additionally, it is clear (Figure 4C) that the  $X$  lines two-dimensional inversions, combined in a quasi-three-dimensional mode, failed to reconstruct the features parallel to the  $X$  axis and they only managed to delineate the structures extended parallel to  $Y$  axis (i.e. vertical to the direction of the  $X$ -line tomographies). A similar result is obtained if the two-dimensional tomographies parallel to the  $Y$  axis are considered, as structures along  $Y$  axis were not reconstructed. Only when both  $X$  and  $Y$  tomographies are combined in a quasi-three-dimensional mode are the structures clearly defined. Concluding, if dense parallel two-dimensional lines (with interline spacing equal to the basic interelectrode spacing) for resistivity tomographies are to be processed with a two-dimensional inversion algorithm, then it is necessary to conduct the survey along both the  $X$  and  $Y$  axes, so as to ensure that no feature details will be 'missed'.

In contrast, this is not the case if the synthetic tomographic data were to be processed using a full three-dimensional inversion algorithm. The inversion procedure for all the three data sets ( $X$ ,  $Y$  and  $XY$  surveys) was completed after 8–10 iterations and the RMS misfit was less than 0.4%. The depth slices show that the three-dimensional resistivity models were fully reconstructed from the original data and they are practically identical for the  $X$ , the  $Y$  and the  $XY$  survey, whereas they seem to be a little more superior from the result obtained by the combined  $XY$  quasi-three-dimensional inversion (Figure 4D). Furthermore, the reconstructed models do not suffer from the artefacts encountered in the two-dimensional  $X$  and  $Y$  inversion procedure, owing to the three-dimensional nature of the bodies.

The synthetic three-dimensional resistivity data sets were contaminated with high levels of Gaussian noise (7%) and then processed with both the two-dimensional and the three-dimensional inversion algorithms. The added

noise was an additional obstacle to the two-dimensional inversion to adequately reconstruct the model, even if the measurements along both axes are considered (Figure 5A). In contrast, the three-dimensional inversion managed to outline the shape, the position and the burial depth of the structures with great accuracy (Figure 5B).

The second model consists of one rectangular prismatic body with a  $200 \Omega\text{-m}$  resistivity and its sides have a dip in relation to the axes. The background resistivity was set equal to  $10 \Omega\text{-m}$ . Although the two-dimensional  $XY$  lines seem to be superior in relation to the two-dimensional  $X$  and the two-dimensional  $Y$  lines, the two-dimensional inversion along the  $X$  or  $Y$  axis reconstructed the original model more successfully than the model of the previous case (Figure 6A). This is obviously due to the fact that the sides of the buried feature were not parallel to the axes but they had a dip in relation to them. Again the application of the three-dimensional inversion algorithm to the data accurately located the structure (Figure 6B), even in the case of very noisy data as depicted in Figure 6C.

The above signify that if a three-dimensional inversion scheme is used then taking measurements only along one direction ( $X$  or  $Y$ ) seems to be adequate to represent the distribution of the subsurface resistivity.

## Real data

The two-dimensional and three-dimensional inversion algorithms were applied to real data in order to verify the results obtained for the synthetic data-sets. The resulting quasi-three-dimensional and three-dimensional resistivity models were compared in respect of the measuring directions. The data sets were collected from two different archaeological sites in Greece. The first test site (Sikyon) is located at the Peloponese (southern Greece), whereas the second site (Europos) lies in northern Greece (Figure 7).

### *Sikyon archaeological site*

The geophysical campaign at the archaeological site of Sikyon (Southern Greece) was conducted by the Laboratory of Geophysical-Remote Sensing

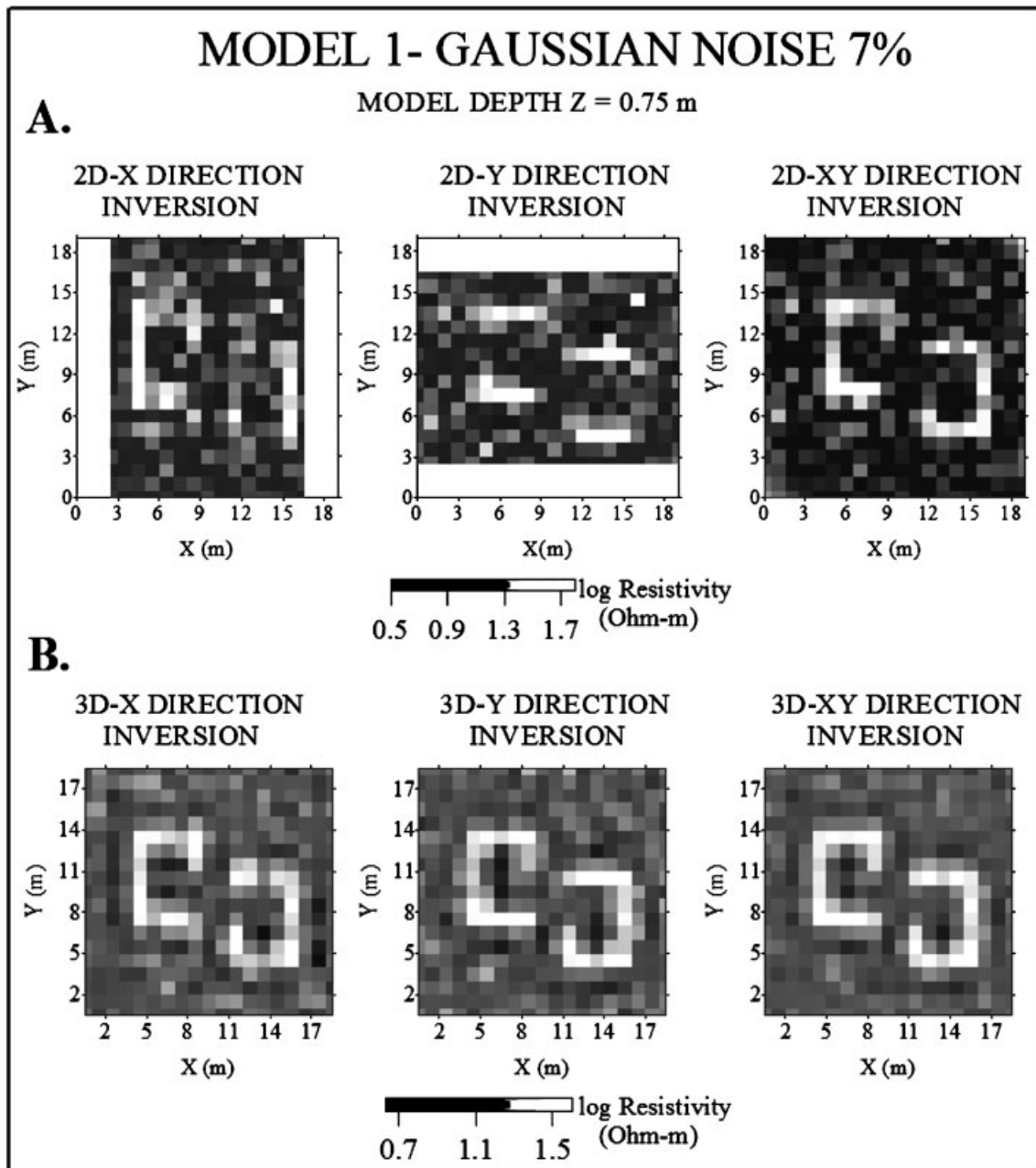


Figure 5. Depth slice at 0.75 m resulting from the two-dimensional (A) and three-dimensional (B) resistivity inversion for the data sets of model 1, which were contaminated with 7% Gaussian noise.

and Archaeoenvironment (I.M.S.-F.O.R.T.H) in October of 2004. An area of 10 800 m<sup>2</sup> was covered using both electrical resistance and magnetic techniques (Sarris, 2004).

A 15 × 10 m rectangular grid was selected from the area and was surveyed using the multiplexed

resistivity system of the Geoscan. The grid was investigated along X and Y axes according to the procedure described in the previous 'instrumentation' section. Twenty-one and thirty-one two-dimensional lines with the pole-pole array, parallel to X and Y axes were collected with

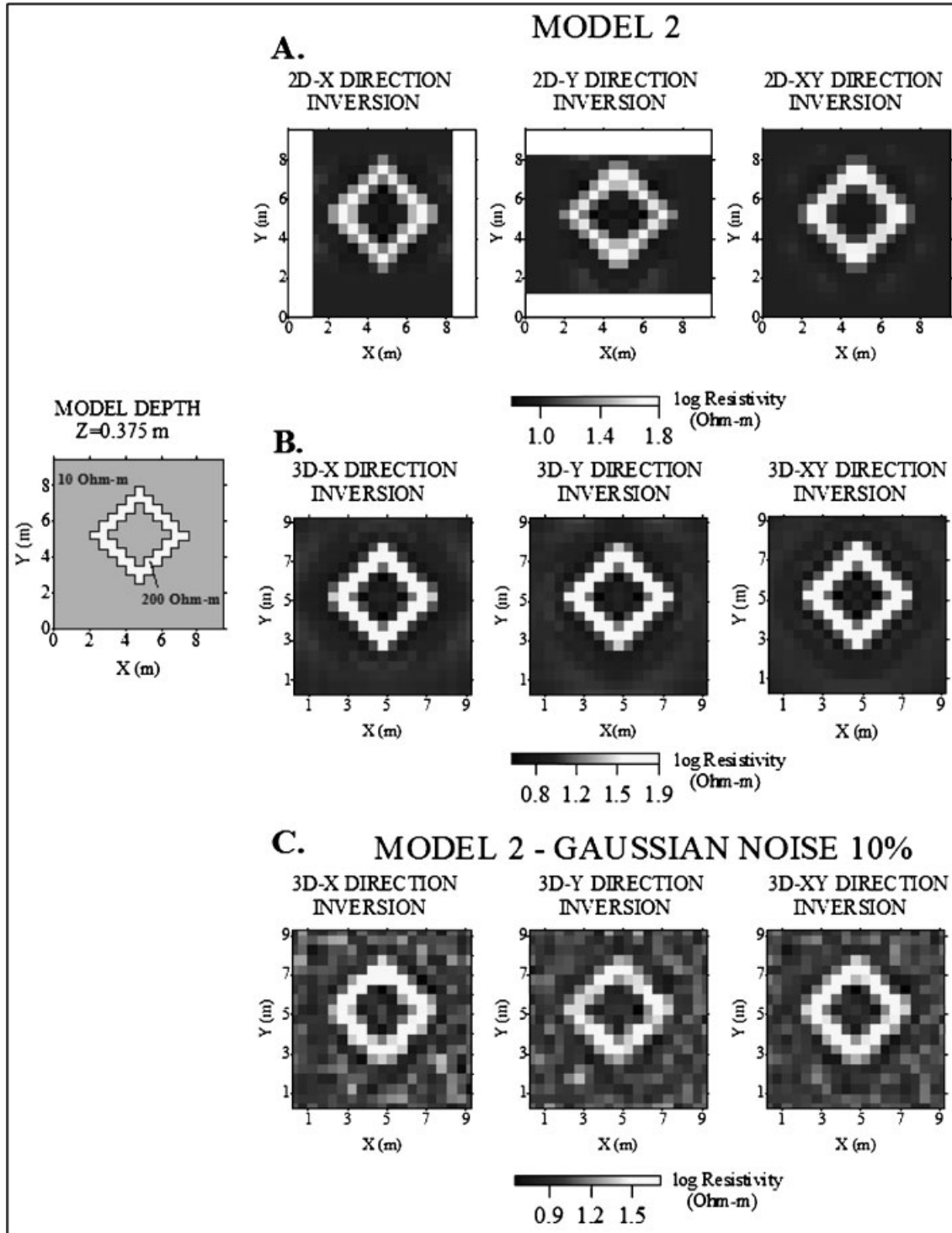


Figure 6. Two-dimensional and three-dimensional resistivity inversion for model 2.

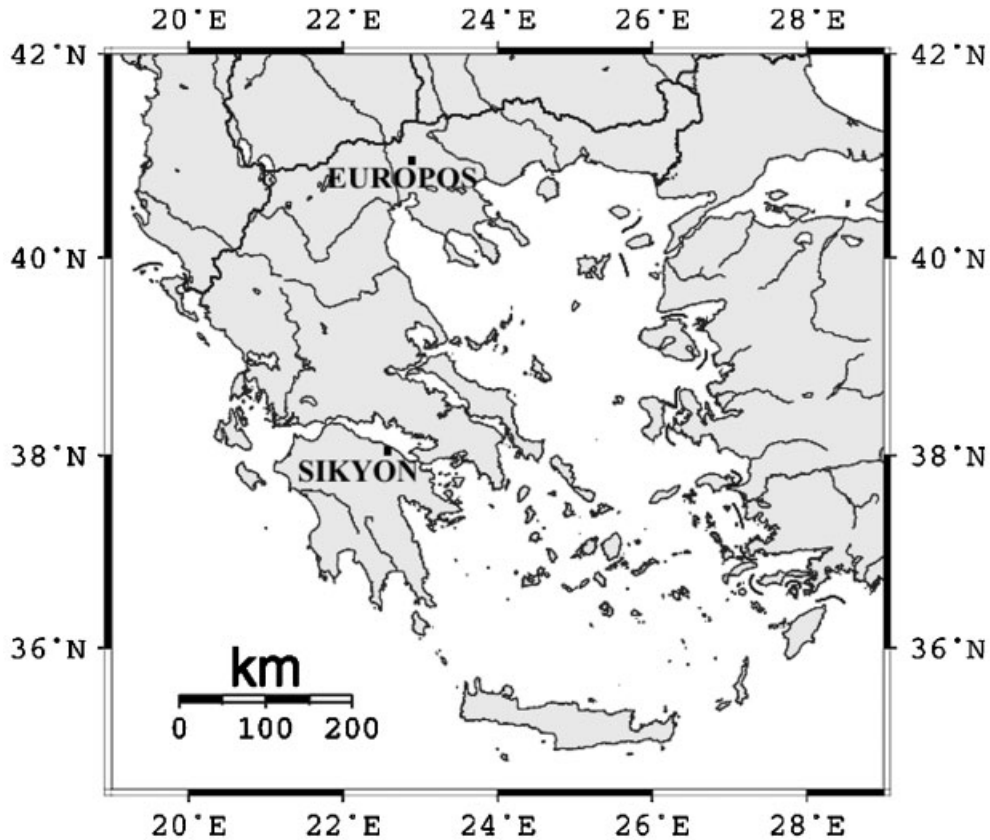


Figure 7. Map of Greece showing the archaeological sites of Sikyon and Europos.

maximum electrode separation  $N_{\max} = 4a$  (where  $a = 0.5$  m). It took about 6 h of field work by two persons to gather these tomographic data, which consisted of approximately 5000 data points. The ground was flat and quite smooth, which facilitated good ground contact of all five electrodes of the frame, in order to record simultaneously the four resistance measurements at each reading station of the grid.

After outlier rejection, every ERT line was inverted separately using the two-dimensional inversion algorithm. All the inversions were stopped at a similar RMS error (2%) in order to reduce variable misfit-induced artefacts when combining results in a quasi-three-dimensional mode.

The results from the two-dimensional inversion along the  $X$ ,  $Y$  and  $XY$  axes were combined so as to produce a quasi-three-dimensional

volume of the subsurface resistivity distribution. Figure 8 shows the four slices of increasing depth that resulted from the quasi-three-dimensional processing of the inverted two-dimensional  $X$ ,  $Y$  and  $XY$  sections respectively.

The reconstructed models ( $X$ ,  $Y$  and  $XY$  directions) depict a rectangular shaped positive resistivity anomaly at a depth of 0.375 m. It is clear that the structures causing this anomaly are the remnants of a buried building. Apart from the outline of this feature, the inversion also managed to identify some inner details, such as the small walls parallel to the  $Y$  axis ( $X = 7$  m), which divide this building into two main compartments. This is more clearly indicated in the two-dimensional  $XY$  inversion.

In the next two depth slices ( $z = 0.625$  m,  $z = 0.875$  m) the two-dimensional  $X$  inversion enhances the features parallel to  $Y$  axis and

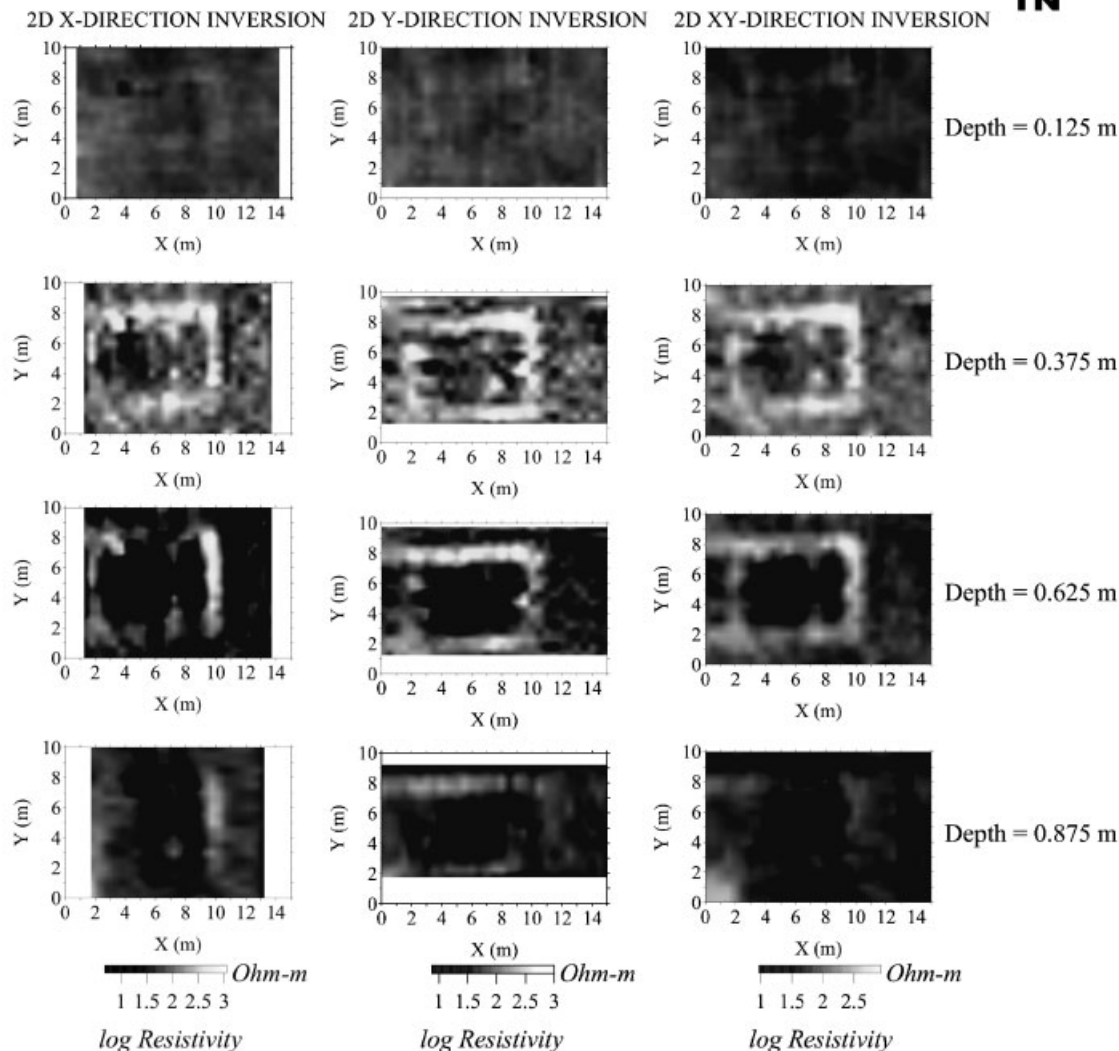
**SIKYON: QUASI-3D RESISTIVITY MODEL**

Figure 8. Quasi-three-dimensional reconstructed models of Sikyon resulting from the two-dimensional X, Y and XY resistivity inversion. The logarithm of the resistivity has been plotted.

missed those that were parallel to X-axis. Exactly the opposite is observed when the Y direction data were processed with the two-dimensional routine. Only when the two-dimensional XY survey is considered are all the sides of the rectangular building depicted. The above example is in full agreement with the conclusions that were made with the synthetic data, as it illustrates the necessity of conducting an XY survey,

if the tomographic data are to be processed with a two-dimensional inversion algorithm.

The independent tomographic data along X, Y and XY directions were combined to three individual data sets corresponding to the three-dimensional X, Y and XY surveys and the non-linear three-dimensional inversion algorithm was used to invert them. The results from the processing of these data are depicted in Figure 9.

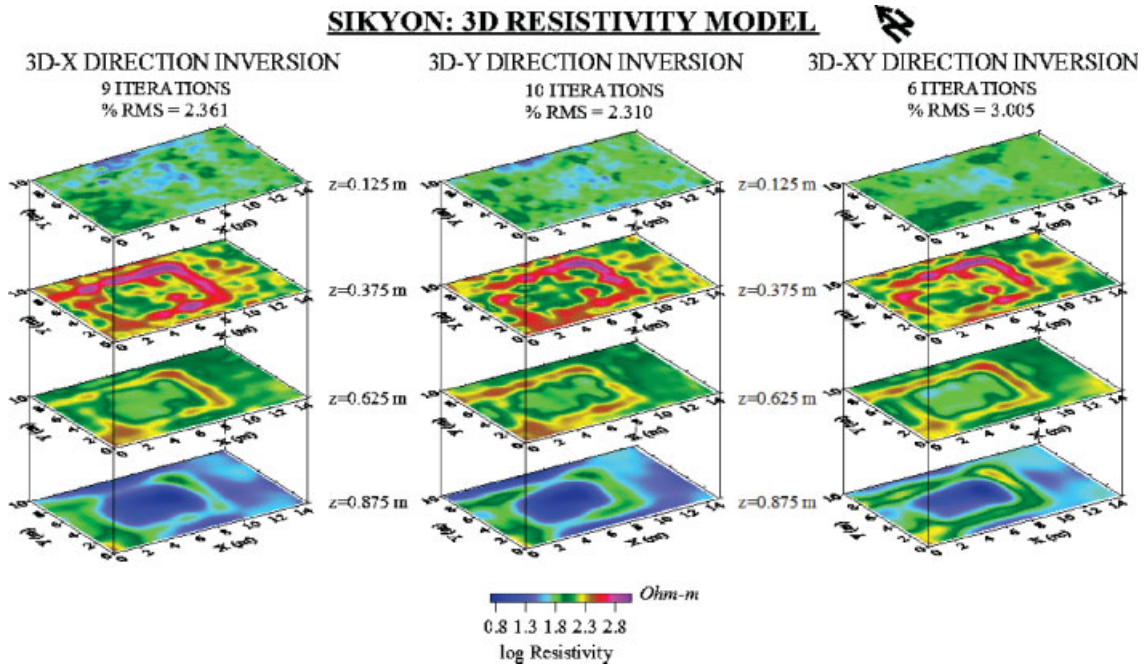


Figure 9. Three-dimensional models of Sikyon resulting from the three-dimensional inversion of the electrical data. The logarithm of the resistivity has been plotted.

The images along X, Y and XY direction are practically identical. The first depth slice ( $z=0.125$  m) seems to have no indication of architectural remnants. As in the two-dimensional inversion case, the outline of an archaeological feature has appeared in the second depth slice ( $z=0.375$  m). The small inner walls parallel to the Y axis, which divide the building into two rooms, can now be identified more clearly in all surveys (X, Y and XY). The basic difference between Figures 8 and 9 is that the three-dimensional inversion (X, Y and XY) reconstructed successfully the shape and the location of the structure in the depth slices from 0.625 m to 0.875 m, without 'losing' any of the features. This indicates the superiority of full three-dimensional images in relation to quasi-three-dimensional ones.

#### *Europos archaeological site*

The field resistivity tomographies were measured using the ABEM Terrameter SAS 4000, along with the Lund imaging automatic system. A  $10 \times 10$  m<sup>2</sup>

square grid was surveyed by conducting 42 two-dimensional parallel lines, 21 along the X axis and 21 along the Y axis, at the archaeological site of Europos (northern Greece). The dipole-dipole configuration was implemented, with the interline and interprobe spacing at 0.5 m. Full details of the survey as well as the two-dimensional and quasi-three-dimensional interpretation of this ERT data are presented by Diamanti *et al.* (2005).

The same processing procedure as in the case of Sikyon was followed. The two-dimensional inversions were stopped at an RMS error of 2.5%. Figure 10 and Figure 11 show the horizontal depth slices of increasing depth for the quasi-three-dimensional and three-dimensional inversion respectively.

A linear anomaly of low resistivity, along the line  $Y=7$  m, appears in the first depth slice ( $z=0.125$  m) of the two-dimensional Y and XY inversions. This anomaly was not reconstructed by the X-line tomographies as it is parallel to their direction. Some features related with archaeological ruins make their appearance as high resistivity values in the second depth layer, mainly in the XY inversion ( $z=0.375$  m). These

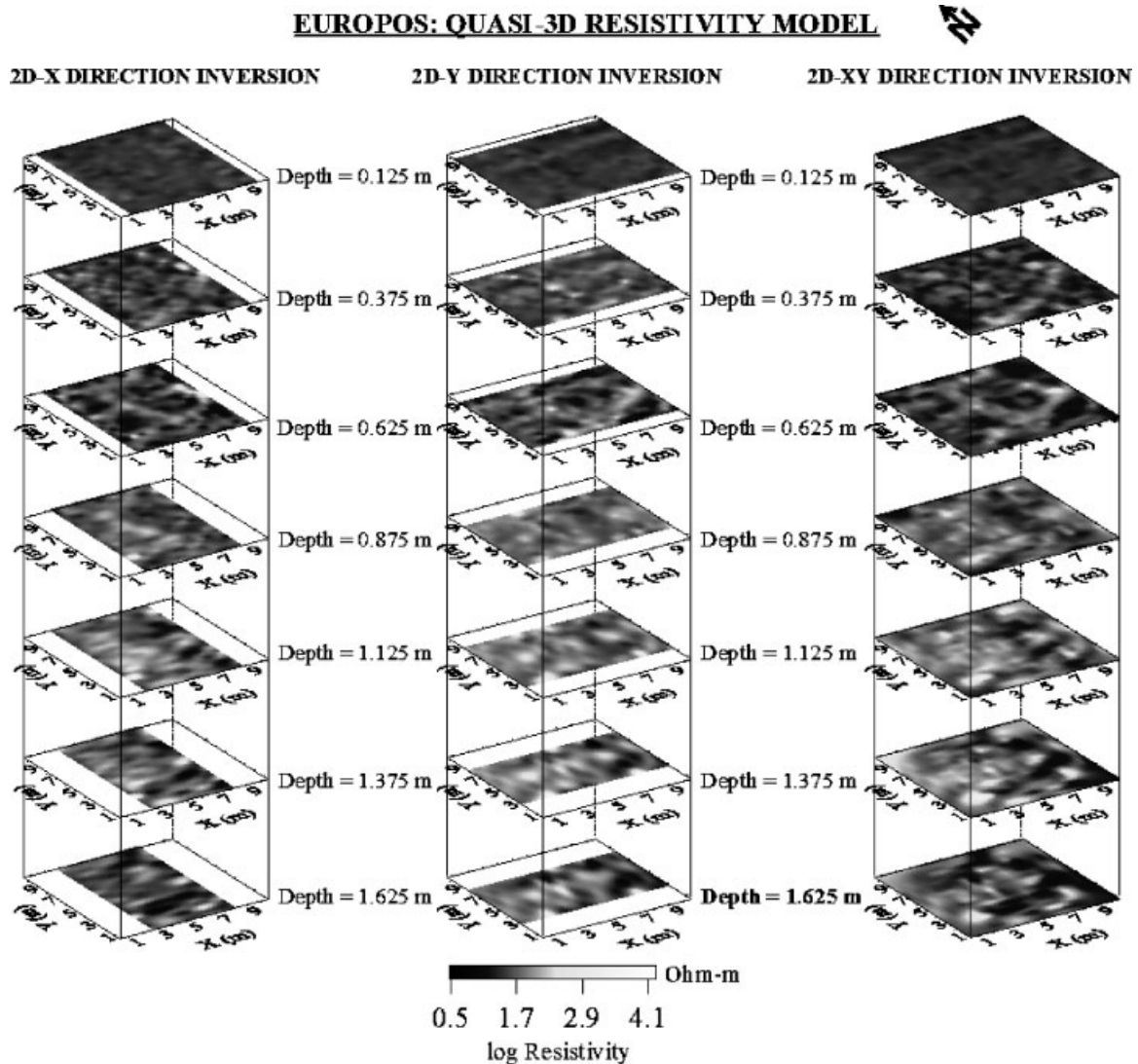


Figure 10. Reconstructed quasi-models from the two-dimensional inversion of the data from the Europos site. The logarithm of the resistivity has been plotted.

continue in the next depth slice ( $z = 0.625$  m) where the diagrammatic interpretation of these linear positive anomalies are shown in Figure 12. Diamanti *et al.* (2005) suggest that the two-dimensional X and XY images are far more informative than the two-dimensional Y image, as the two-dimensional Y inversion failed to locate the structures that were oriented almost parallel to Y axis. The remaining depth slices show regions with high resistivity values, probably related to buried relics, but unfortunately

these regions do not form a regular geometric shape.

Once more the three-dimensional inversion gave superior results in relation to the two-dimensional one. The reconstructed images are very similar for the three-dimensional X, Y and XY direction surveys and the RMS of the models was quite low (3.3–4.6%). The buried feature begins to appear at a depth of 0.375 m with a few scattered remnants, it is fully formatted at a depth of 0.625 m and continues until a depth of

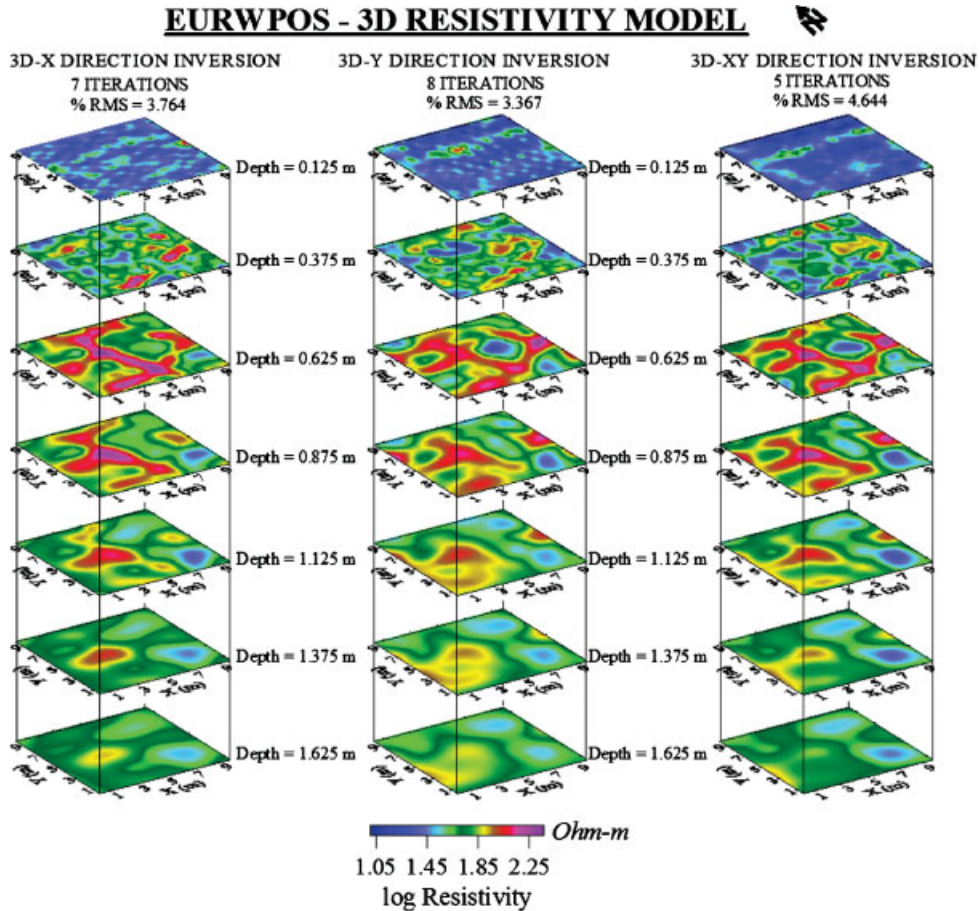


Figure 11. Variation of the ground resistivity in three dimensions from the Europos archaeological site. The logarithm of the resistivity has been plotted.

approximately 1 m, where it seems to fade away. Probably the located structure comprises the remnants of the walls of a buried building, which seems to be divided into three different rooms. It is also worth noting that the low resistivity linear anomaly in the first depth layer (centred at 0.125 m) is now delineated by the X-inversion as well. Furthermore, the three-dimensional Y (and XY) inversion indicates that the buried structure may continue to the west. This continuation is not suggested by the three-dimensional X inversion due to the gradually poorer horizontal coverage at the east and west edges that the parallel tomographies have, as the depth increases.

Figure 12 shows a comparison of the recorded features from the depth layer centred at 0.625 m,

using the two-dimensional X, Y, XY and the three-dimensional Y surveys, which indicates the superiority of the three-dimensional inversion. Only when the survey has been conducted along both axes does the quasi-three-dimensional inversion gave identical results to the three-dimensional one.

## Conclusions

The investigation and mapping of archaeological sites by conducting full three-dimensional resistivity measurements is a very time-consuming procedure as a large number of field measurements have to be gathered. Nowadays, modern

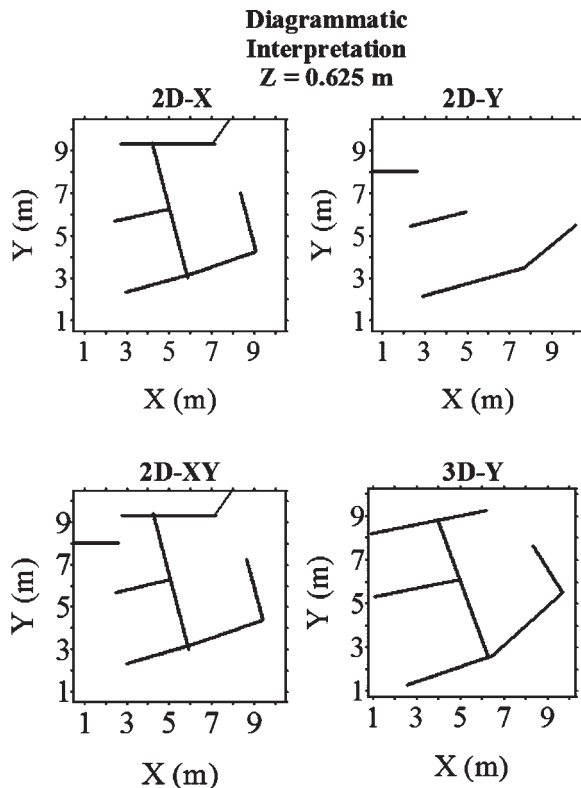


Figure 12. Diagrammatic interpretation of the recorded anomalies from the depth of 0.625 m for the two-dimensional X, Y, XY and three-dimensional Y surveys.

and fully automated multiplexed resistivity meters have been developed, reducing the overall field time, but again such surveys have not been used on a routine basis so far.

In order to record the distribution of the earth resistivity in archaeological areas in three dimensions, alternative measuring modes must be used. These modes must compromise speed, low cost and adequate vertical and horizontal coverage. The gathering of resistivity data in parallel tomographies constitutes the most common field practice nowadays.

The first question that arises in this case concerns the optimum survey direction. Do the measurements have to be conducted along X, along Y or along the both of the axes? And then, how should these data be interpreted? Are two- or three-dimensional inversion algorithms able to reconstruct adequately the resistivity distribution and what are the main differences between them?

The results in synthetic data showed that quasi-three-dimensional images suffered from artefacts because the three-dimensional archaeological features are approached as varying only in two dimensions. Only the combination of an XY survey with two-dimensional inversion and quasi-three-dimensional presentation can give satisfactory results.

In contrast, the three-dimensional inversion algorithms gave practically identical results for the three-dimensional X, Y and XY surveys and obviously they were superior in relation to the two-dimensional ones. These illustrate that dense parallel lines across X or Y directions combined with three-dimensional schemes are adequate to reconstruct the buried structures. Furthermore the three-dimensional algorithm seems to work equally well even in the presence of very noisy data.

The application of the algorithms to real data collected from two different archaeological regions proved and verified the observations made with the synthetic data. It also established the effectiveness of the three-dimensional routines in the reconstruction of complicated structures (Europos example), even when measurements from only one direction are considered.

In summary, the combination of gathering parallel tomographic data in one direction and processing them via three-dimensional schemes can be a useful tool in the geophysical investigations of archaeological sites, as the burial depth, the location and the depth extent of potential architectural remnants can be recorded accurately. This approach of combining dense two-dimensional measurement with three-dimensional inversion is considered practical for routine data treatment because the extra computational time/power required by three-dimensional inversion schemes is compensated by the reduced amount (50% less) of field data required when compared with the quasi-three-dimensional approach.

Further, it is shown that by simple modification of standard archaeological survey equipment, tomographic three-dimensional data sets can be obtained efficiently. It is clear that this approach is not necessarily applicable to routine archaeological site surveying but can be used in combination and after the standard

electrical profiling in areas that exhibit structures and which deserve further and more detailed investigation.

## Acknowledgements

Nikos Papadopolous would like to thank the Greek State Scholarships Foundation (GSSF) for their financial support of this work.

## References

- Aspinall A, Gaffney CF. 2001. The Schlumberger array-potential and pitfalls in archaeological prospecting. *Archaeological Prospection* **8**: 199–209.
- Atzemoglou A, Tsourlos P, Pavlides S. 2003. Investigation of the tectonic structure of the NW part of the Amynteon Basin (NW Greece) by means of a vertical electrical sounding (VES) survey. *Journal of the Balkan Geophysical Society* **6**(4): 188–201.
- Burnett DS. 1988. *Finite Element Analysis (from concept to applications)*. Addison-Wesley: AT&T Laboratories: New Jersey.
- Çaglar I, Duvarci E. 2001. Geoelectric structure of inland area of Gökova rift, southwest Anatolia and its tectonic implications. *Journal of Geodynamics* **31**: 33–48.
- Chambers JE. 2001. *The application of 3D electrical tomography to the investigations of brownfield sites*. PhD thesis, University of Sheffield.
- Chouker F. 2001. Archaeological site investigation by geoelectrical measurements in Tel-Halawi (northern Syria). *Archaeological Prospection* **8**: 257–263.
- Clark A. 1990. *Seeing Beneath the Soil-Prospection Methods in Archaeology*. B.T. Batsford: London.
- Constable SC, Parker RL, Constable CG. 1987. Occam's inversion: a practical algorithm for generating smooth models from electromagnetic sounding data. *Geophysics* **52**(3): 289–300.
- Coggon JH. 1971. Electromagnetic and electrical modelling by the finite element method. *Geophysics* **36**(1): 132–155.
- Dabas M, Hesse A, Tabbagh J. 2000. Experimental resistivity survey at Wroxeter archaeological site with a fast and light recording device. *Archaeological Prospection* **7**: 107–118.
- Dahlin T, Loke MH. 1997. Quasi-3D resistivity imaging-mapping of three dimensional structures using two dimensional DC resistivity techniques. *Proceedings of the 3rd Meeting of the Environmental and Engineering Geophysics*; 8–11 September 1997, Aarhus, Denmark; 143–146.
- Dahlin T, Owen R. 1998. Geophysical investigations of alluvial aquifers in Zimbabwe. *Proceedings of the IV Meeting of the Environmental and Engineering Geophysical Society (European Section)*, September, Barcelona; 151–154.
- Dahlin T, Johansson S, Landlin O. 1994. Resistivity surveying for planning of Infrastructure. *Proceedings of Symposium on the Application of Geophysics to Engineering and Environmental Problems* 27–31 March, Boston, Massachusetts; 509–528.
- De groot-Hedlin C, Constable S. 1990. Occam's inversion to generate smooth, two-dimensional models from magnetotelluric data. *Geophysics* **55**: 1613–1624.
- Diamanti N, Tsokas G, Tsourlos P, Vafidis A. 2005. Integrated interpretation of geophysical data in the archaeological site of Europos (northern Greece). *Archaeological Prospection* **12**: 79–91.
- Dogan M, Papamarinopoulos S. 2003. Geoelectric prospecting of a city wall by multi-electrode resistivity image survey at the prehistoric site of Asea (southern Greece). *Archaeological Prospection* **10**: 241–248.
- Ellis R, Oldenburg DW. 1994. Applied geophysical inversion. *Geophysical Journal International* **116**: 5–11.
- Flathe H. 1955. Possibilities and limitations in applying geoelectrical methods to hydrogeological problems in the coastal areas of Northwest Germany. *Geophysical Prospecting* **3**: 95–110.
- Gaber S, El-Fiky AA, Abou Shagar A, Mohamaden M. 1999. Electrical resistivity exploration of the Royal Ptolemaic Necropolis in the Royal Quarter of Ancient Alexandria, Egypt. *Archaeological Prospection* **6**: 1–10.
- Loke MH, Barker RD. 1995. Least-squares deconvolution of apparent resistivity pseudosections. *Geophysics* **60**(6): 1682–1690.
- Loke MH, Barker RD. 1996. Practical techniques for 3D resistivity surveys and data inversion. *Geophysical Prospecting* **44**: 499–523.
- McGillivray P, Oldenburg D. 1990. Methods for calculating Fréchet derivatives and sensitivities for the non-linear inverse problem: a comparative study. *Geophysical Prospecting* **38**: 499–524.
- Neighbour T, Strachan R, Hobbs BA. 2001. Resistivity imaging of the linear earthworks at the Mull of Galloway, Dumfries and Galloway. *Archaeological Prospection* **8**: 157–162.
- Noel M. 1991. *Multielectrode Resistivity Tomography for Imaging Archaeology*. British Archaeological Reports: Oxford.
- Paige C, Saunders M. 1982. LSQR: an algorithm for sparse linear equations and sparse least squares. *ACM Transactions on Mathematical Software* **8**: 43–71.
- Panissod C, Dabas M, Hesse A, Jolivet A, Tabbagh J, Tabbagh A. 1998. Recent developments in shallow-depth electrical and electrostatic prospecting using mobile arrays. *Geophysics* **63**(5): 1542–1550.
- Park SK, Van GP. 1991. Inversion of pole-pole data for 3-D resistivity structures beneath arrays of electrodes. *Geophysics* **56**: 951–960.

- Press WH, Teukolsky SA, Vetterling WT, Flannery BP. 1992. *Numerical Recipes in C: The Art of Scientific Computing*, 2nd edn. Cambridge University Press: Cambridge.
- Pridmore DF, Hohmann GW, Ward SH, Sill WR. 1981. An investigation of finite-element modeling for electrical and electromagnetic data in three dimensions. *Geophysics* **46**(7): 1009–1024.
- Ramirez A, Daily W, Binley A, Labrecque D. 1996. Tank leak detection using electrical resistance methods. *Symposium on the Application of Geophysics to Engineering and Environment*, Keystone, CO; 28 April–1 May.
- Rijo L. 1977. *Modeling of electric and electromagnetic data*. PhD thesis, University of Utah.
- Rizzo E, Chianese D, Lapenna V. 2005. Magnetic, GPR and geoelectrical measurements for studying the archaeological site of “Masseria Nirgo” (Viggiano, southern Italy). *Near Surface Geophysics* **3**(1): 13–19.
- Rogers RB, Kean WF. 1980. Monitoring ground water contamination at a fly ash disposal site using surface resistivity methods. *Ground Water* **18**(5): 472–478.
- Sarris A. 1992. *Shallow depth geophysical investigation through the application of magnetic and electric resistance techniques: an evaluation study of the responses*. PhD thesis, University of Nebraska: Lincoln.
- Sarris A. 2004. *Preliminary Report of the Geophysical Investigations in the Archaeological Site of Sikyon*. Institute for Mediterranean Studies: Rethimno, Crete, 29 pp. (In Greek).
- Sarris A, Topouzi S, Adrimi-Sismani V. 2002. Mycenaean Dimini: integration of geophysical surveying and GIS. *CAA2002 International Conference: Computer Applications & Quantitative Methods in Archaeology. The Digital Heritage of Archaeology*. Herakleion, Crete, 2–6 April.
- Sasaki Y. 1992. Resolution of resistivity tomography inferred from numerical simulation. *Geophysical Prospecting* **40**: 453–464.
- Tsokas GN, Giannopoulos A, Tsourlos P, Vargemzis G, Tealby JM, Sarris A, Papazachos CB, Savopoulou T. 1994. A large scale geophysical survey in the archaeological site of Europos (northern Greece). *Journal of Applied Geophysics* **32**: 85–98.
- Tsourlos P. 1995. *Modelling interpretation and inversion of multielectrode resistivity survey data*. Unpublished PhD thesis, University of York.
- Tsourlos P, Ogilvy R. 1999. An algorithm for the 3-D inversion of tomographic resistivity and induced polarization data: preliminary results. *Journal of the Balkan Geophysical Society* **2**(2): 30–45.
- Tsourlos P, Szymanski J, Tsokas G. 1999. The effect of terrain topography on commonly used resistivity arrays. *Geophysics*, **64**: 1357–1363.
- Vafidis A, Sarris A, Sourlas G, Ganiatsos Y. 1999. Two and three dimensional electrical tomography investigations in the archaeological site of Itanos, Crete, Greece. *Second Balkan Geophysical Congress and Exhibition*, Istanbul, 5–9 July.
- Van PV, Park SK, Hamilton P. 1991. Monitoring leaks from storage ponds using resistivity methods. *Geophysics*. **56**: 1267–1270.
- Walker AR. 2000. Multiplexed resistivity survey at the roman town of Wroxeter. *Archaeological Prospection* **7**: 119–132.
- Xu B, Noel M. 1993. On the completeness of data sets with multielectrode systems for electrical resistivity survey. *Geophysical Prospecting* **41**: 791–801.